2.E Nuclear Physics A208 (1973) 333—359; © North-Holland Publishing Co., Amsterdam

CALCULATION OF THE IMAGINARY PART OF THE NUCLEON-NUCLEUS OPTICAL-MODEL POTENTIAL

J. CUGNON †

Physique Nucléaire Théorique, Institut de Physique,
Université de Liège, Sart-Tilman, B-4000 Liège 1, Belgique

Received 27 December 1972
(Revised 5 March 1973)

Abstract: The imaginary part of the optical-model potential for the scattering of nucleons by nuclei is studied in the frame of the shell-model approach to nuclear reactions. Special attention is paid to the one-hole target nuclei. The imaginary part of the optical-model potential in the second order in the nucleon-nucleus interaction is divided into two parts. The first corresponds to the average resonant scattering. The second corresponds to the inelastic scattering leading to the non-collective states of the target nuclei. A local potential equivalent to the non-local theoretical one is constructed in order to facilitate comparison with experiment. Numerical calculations concern the scattering of 14.5 MeV protons by ^{39}K. It is found that the imaginary part depends upon the angular momentum and that its radial variation is governed by strong shell effects. The predicted absorption is approximately 60% of the experimental one. The average resonant scattering contributes to the imaginary part of the optical-model potential as much as the inelastic non-collective excitations of the target.

1. Introduction

A microscopic calculation of the imaginary part of the nucleon-nucleus optical-model potential (OMP) is difficult. The reason is that, in the simplest approximation, there are many intermediate states to take into account. In general, one does not know the nature of most of these states. Therefore, the imaginary part of the OMP has been calculated only in phenomenological models, like the Fermi gas model [1]), or the Thomas-Fermi approximation [2-4]), except for several recent investigations [refs. [5-7])]. However, these are incomplete to a large extent. Either they stop at the construction of the non-local potential, or they do not include the contribution of the averaging procedure. Indeed, we recall that the imaginary part of the OMP comes not only from the excitation of the inelastic channels, but also from average elastic resonant scattering. Let S_{cc} be the scattering matrix of the total system in a given elastic channel c. The OMP in this channel is associated with a scattering function equal to the average of S_{cc} on some interval I: $\langle S_{cc} \rangle_I$. This quantity is not unitary, if inelastic channels are open or if S_{cc} is energy dependent. Thus, the average resonant scattering contributes to the absorption, but it has been neglected in previous investigations, with the exception of its partial treatment in ref. [7]).

† Chercheur IISN. This work is partly based on the Ph.D. thesis of the author.

Our purpose is to study the OMP, and especially its imaginary part, in the frame of the shell-model theory of nuclear reactions [9]). In particular, we compare the contributions of the average resonant scattering (we shall say the compound nucleus contribution) and of the inelastic scattering, respectively, to the absorption. We then construct a local potential which is equivalent to the non-local potential that we have calculated. We compare with experiment the cross sections derived from both potentials, and the equivalent local potential itself. Finally, we investigate the non-locality of the calculated theoretical potential.

For the sake of convenience, we restrict the model space to particle-hole states. Thus, we choose targets whose states are well described by the shell model. One-hole nuclei may fulfil this requirement. Our numerical calculations concern the scattering of protons by ^{39}K, for which the OMP is known at 14.5 MeV incident energy [10]). We introduce explicitly all the 1p-1h configurations of the total system which are necessary for the calculation. The more complicated configurations are implicitly taken into account through the spreading width of the 1p-1h resonant states.

We briefly summarize some of our results. Firstly, the compound states contribution to the absorption is of the same size as the contribution of the inelastic excitation of the non-collective target states. However, the total contribution (compound states plus non-collective target excitations) is too small, by about 40 %. Secondly, the imaginary part of the OMP contains a large volume component. The most striking result is the appearance of shell effects both in the radial variation of the imaginary part of the OMP and in the variation of the non-locality parameter. Those shell effects can be related to the fact that the excitation of particles from below to above the Fermi sea is favourably initiated, during collisions with the incident nucleon, where the overlap of the matter density in the shells above and below the Fermi sea is important.

In sect. 2, we briefly recall the expression of the OMP in the frame of the shell model. Sect. 3 is devoted to the definition of the model space and to some consequences of this definition for the calculation. In sect. 4, we give the details of the calculation and the results in the form of some quantities, specifying the non-local theoretical imaginary part of the OMP. Sect. 5 is divided into two parts. Firstly, we construct a local potential equivalent to the non-local theoretical one. Secondly, we compare both this equivalent potential and the cross sections derived from it to the experimental data. In sect. 6, we investigate the non-locality of the theoretical OMP. Sect. 7 contains a discussion on the predicted localization and intensity of the absorption. We give the conclusions in sect. 8.

2. Optical-model potential and the shell-model in the continuum

In this section, we define the notation, we recall the formula of the optical-model potential for a given channel, and we derive the expression of the optical-model potential for an incident plane wave.

2.1. THE SHELL MODEL IN THE CONTINUUM

The total Hamiltonian is divided into two parts:

$$H = H_0 + V, \tag{2.1}$$

$$H_0 = \sum_i h_0(i) = \sum_i (t(i) + v_0(i)), \tag{2.2a}$$

$$V = \sum_{i<j} v(i, j) - \sum_i v_0(i). \tag{2.2b}$$

In these relations, $v(i,j)$ is the interaction between the two nucleons i, j and v_0 is the average model potential well. This real potential well has a finite depth. We denote its bound and scattering states by $w_{lj}(r, k_n)$ and $u_{lj}(r, k)$ respectively †.

The Hamiltonian H_0 possesses bound states ϕ_i and scattering states χ_E^c with only one nucleon in a scattering state $u_{lj}(r, k_c)$. We have the following expressions and definitions:

$$H_0 \phi_i = E_i \phi_i, \quad H_0 \chi_E^c = E \chi_E^c, \quad E = \varepsilon_c + \hbar^2 k_c^2 / 2M, \tag{2.3}$$

ε_c being the threshold for the channel c.

2.2. THE OPTICAL-MODEL POTENTIAL FOR A GIVEN CHANNEL c

One can write the optical-model wave function in channel c [ref. [9])] as:

$$\tilde{\rho}_E^c(r) = \int_{\varepsilon_c}^{\infty} \tilde{a}_E^c(c, E') u_c(r, k_c') \, \mathrm{d}E'. \tag{2.4}$$

The Schrödinger equation [9]) is:

$$(E - D_{lj}) \tilde{\rho}_E^c(r) - \int_0^{\infty} \tilde{\mathscr{V}}_E^c(r, r') \tilde{\rho}_E^c(r') \, \mathrm{d}r' = 0, \tag{2.5}$$

where D_{lj} is the radial component of $h_0 = t + v_0$. This equation is equivalent to the following one:

$$(E - E') \tilde{a}_E^c(c, E') - \int_{\varepsilon_c}^{\infty} \tilde{\mathscr{V}}_E^c(E', E'') \tilde{a}_E^c(c, E'') \, \mathrm{d}E'' = 0, \tag{2.6}$$

with [9])

$$\tilde{\mathscr{V}}_E^c(E', E'') = \int_0^{\infty} \mathrm{d}r \int_0^{\infty} \mathrm{d}r' u_c(r, k_c') \tilde{\mathscr{V}}_E^c(r, r') u_c(r', k_c''), \tag{2.7}$$

$$\tilde{\mathscr{V}}_E^c(r, r') = \int_{\varepsilon_c}^{\infty} \mathrm{d}E' \int_{\varepsilon_c}^{\infty} \mathrm{d}E'' u_c(r, k_c') \tilde{\mathscr{V}}_E^c(E', E'') u_c(r', k_c''). \tag{2.8}$$

The quantities $\tilde{\mathscr{V}}_E^c(E', E'')$ and $\tilde{\mathscr{V}}_E^c(r, r')$ are the shell model and r-representation of $\tilde{\mathscr{V}}_E^c$ respectively. When there are no single-particle resonances in the vicinity of the energy of interest, the whole optical-model potential in channel c (OMP(c)) is given [refs. [9, 11])] by:

$$\mathscr{V}_E^{\mathrm{opt}(c)} = v_0 + \tilde{\mathscr{V}}_E^c(r, r') = v_0 + \mathscr{V}_{E+iI}^c(r, r'), \tag{2.9}$$

† For the conventions, see ref. [9]) ch. I.

I being the averaging interval.

The general expression for the quantity $\mathscr{V}_E^c$ is

$$\mathscr{V}_E^c(E', E'') = \langle\chi_{E'}^c|V_{\text{eff}}|\chi_{E''}^c\rangle + \sum_{s,s'}\langle\chi_{E'}^c|V_{\text{eff}}|\phi_s\rangle\langle\phi_s|[E+iI-H_0-V_{\text{eff}}]^{-1}|\phi_{s'}\rangle\langle\phi_{s'}|V_{\text{eff}}|\chi_{E''}^c\rangle, \tag{2.10}$$

with

$$V_{\text{eff}} = V + V\frac{Q_c}{E^+-H_0}V_{\text{eff}}, \tag{2.11a}$$

$$Q_c = \sum_{c'\neq c}\int_{\varepsilon_{c'}}^{\infty} dE'\chi_{E'}^{c'}\rangle\langle\chi_{E'}^{c'}. \tag{2.11b}$$

In second order in V, the OMP(c) is given in r-representation by:

$$\mathscr{V}_E^{\text{opt}(c)}(r, r') = v_0 + \mathscr{V}_E^{\text{CN}}(r, r') + \mathscr{V}_E^{\text{DIR}}(r, r'), \tag{2.12a}$$

$$\mathscr{V}_E^{\text{CN}}(r, r') = \sum_s \langle\chi_r^c|V|\phi_s\rangle(E+iI-E_s)^{-1}\langle\phi_s|V|\chi_{r'}^c\rangle, \tag{2.12b}$$

$$\mathscr{V}_E^{\text{DIR}}(r, r') = \langle\chi_r^c|V|\chi_{r'}^c\rangle + \sum_{c'\neq c}\int_{\varepsilon_{c'}}^{\infty}\langle\chi_r^c|V|\chi_{E'}^{c'}\rangle\frac{dE'}{E^+-E'}\langle\chi_{E'}^{c'}|V|\chi_{r'}^c\rangle, \tag{2.12c}$$

with

$$|\chi_r^c\rangle = \int_{\varepsilon_c}^{\infty} dE' u_c(r, k_c')|\chi_{E'}^c\rangle. \tag{2.12d}$$

2.3. THE OPTICAL-MODEL POTENTIAL FOR AN INCIDENT PLANE WAVE

The OMP(c) defined by eq. (2.9) is the one acting in a given channel c. The latter index covers the following set of quantum numbers: the orbital and total angular momentum quantum numbers of the relative motion l, j, the spin of the target I_c, the total spin of the system J, the isospin of the target T_c and its z-component M_{T_c}, the total isospin T and its z-component M_T. We have to compute the OMP acting on an incident plane wave. We do not want to retain in this work an imaginary spin-orbit term (since in the case we will study such a term has not been included in the phenomenological OMP), nor a spin-spin term, which is very small. Then, as we show in the appendix, the OMP acting on an incident plane wave can be reduced to:

$$\mathscr{V}^{\text{opt}}(\boldsymbol{r}, \boldsymbol{r}') = v_0 + \mathscr{V}^{\text{plane}}(\boldsymbol{r}, \boldsymbol{r}'), \tag{2.13}$$

with

$$\mathscr{V}^{\text{plane}}(\boldsymbol{r}, \boldsymbol{r}') = \sum_L \frac{2L+1}{4R}\frac{\overline{\mathscr{V}}_L(r, r')}{rr'}P_L(\cos\Theta). \tag{2.14}$$

The multipoles $\overline{\mathscr{V}}_L(r, r')$ are given by the relation (see appendix):

$$\overline{\mathscr{V}}_L(r, r') = \sum_j (L0\tfrac{1}{2}\tfrac{1}{2}|j\tfrac{1}{2})^2 \sum_{\mu_I}(2I_c+1)^{-1}\sum_j (j\tfrac{1}{2}I_c\mu_I|J\mu_I+\tfrac{1}{2})^2 \times \sum_T (T_c M_{T_c}\tfrac{1}{2}m_t|TM_T)^2\tilde{\mathscr{V}}_E^{c=\{LjI_cJm_tM_{T_c}TM_T\}}(r, r'), \tag{2.15}$$

with m_t the z-component of the isospin of the incident nucleon. The quantity $\tilde{\mathscr{V}}_E^c$ is given in eq. (2.9).

3. The model space

In order to make the calculation feasible, it is necessary to truncate the configuration space. Since we study the example of a target constituted by a magic nucleus minus one nucleon, we take a model space spanned by the shell-model configuration with n particles and n holes, trying to make n as low as possible in order to simplify the calculations.

As a first step, one can take for the elastic and inelastic channel states 1p-1h configurations: the target states are then obtained by making a hole in the core of the magic nucleus. Such a description is not sufficient for the compound nucleus (CN) states ϕ_s. Indeed, if, in the expressions (2.12b), we only retain the 1p-1h states ϕ_s, the corresponding OMP should generate resonances with a width equal to $2I+2\pi\langle\phi_s|V|\chi_E^c\rangle^2$. This quantity is in general smaller than the average separation between the 1p-1h states. A structure should then remain in the cross sections. Such a structure is not observed experimentally. The reason is that 2p-2h states are coupled to the 1p-1h states, broadening the latter ones. This effect is accounted for by changing eq. (2.12b) into:

$$\mathscr{V}_E^{\mathrm{CN}} = \sum_s \langle\chi_r^c|V|\phi_s\rangle(E+iI_{\mathrm{eff}}-E_s)^{-1}\langle\phi_s|V|\chi_{r'}^c\rangle + \sum_l \langle\chi_r^c|V|\phi_l\rangle(E+iI-E_l)^{-1}\langle\phi_l|V|\chi_{r'}^c\rangle. \qquad (3.1)$$

Here, the index s runs over the 1p-1h states. The second term comes from the contribution of the 2p-2h states. In general, those states are not coupled to the incident channel, because of the structure of χ_E^c. Only those 2p-2h states with one hole identical to the hole of χ_E^c are directly coupled to χ_E^c. The quantity I_{eff} is equal to

$$I_{\mathrm{eff}} = I+\tfrac{1}{2}\overline{\Gamma_s^{\downarrow}}^s. \qquad (3.2)$$

The quantity $\Gamma_s^{\downarrow}$ is the spreading width of the 1p-1h states ϕ_s due to the coupling of the latter to the 2p-2h states. One can find a more rigorous justification of eq. (3.1) in ref. [12]).

It can easily be shown [12]) that, as a consequence of the use of this model space, the real part of the OMP is well described by the Hartree-Fock field. Since we are mainly interested in the imaginary part of the OMP, we shall assume in the following that the potential v_0 gives a good approximation of the Hartree-Fock field, as far as scattering properties are concerned.

4. Calculation and results

We give below the details of the calculation of the imaginary part of the OMP for the case ^{39}K+p. We concentrate our attention on 14 MeV incident protons in the center-of-mass system.

4.1. THE AVERAGE POTENTIAL v_0

We have chosen a potential which reproduces the single-particle scheme for ^{40}Ca [refs. [13,14])]. For the neutrons, v_0 is a Saxon-Woods potential plus a spin-orbit term with the parameters of Takeuchi and Moldauer [15]). For the protons, an additional Coulomb term is introduced and the depth of the central potential is changed. The parameters and the single-particle spectrum are given in table 1.

TABLE 1

Saxon-Woods well parameters and single-particle energies

	Neutron [a])	Proton [b])
$2p_{\frac{1}{2}}$	− 1.1781	unbound
$2p_{\frac{3}{2}}$	− 4.0077	− 1.0090
$1f_{\frac{7}{2}}$	− 7.9714	− 5.4205
$1d_{\frac{3}{2}}$	−12.3779	−10.0872
$2s_{\frac{1}{2}}$	−13.4495	−10.8055
$1d_{\frac{5}{2}}$	−17.5685	−15.2441
$1p_{\frac{1}{2}}$	−24.3078	−22.1148
$1p_{\frac{3}{2}}$	−26.7565	−24.5502
$1s_{\frac{1}{2}}$	−35.2841	−33.0469

[a]) $V_0 = 46$ MeV, $V_{s.o.} = 9.5$ MeV, $r_0 = 1.16$ fm, $a = 0.62$ fm, $r_1 = 0.60$ fm, $R_0 = r_0 A^{\frac{1}{3}} + r_1$.
[b]) $V_0 = 52.3$ MeV, $V_{s.o.} = 9.5$ MeV, $r_0 = 1.16$ fm, $a = 0.62$ fm, $R_0 = r_0 A^{\frac{1}{3}} + r_1$, $R_{Coul} = R_0$, $r_1 = 0.60$ fm.

The ground state of ^{40}Ca is obtained by filling the levels up to $1d_{\frac{3}{2}}$ with both protons and neutrons. Owing to the small isovector component of v_0, isospin is not a good quantum number for ^{40}Ca. However, we shall assume that we have a pure $T = 0$ state. This approximation is justified, since the overlap of the wave function for conjugate single-particle states is larger than 0.99 for the levels below and above the Fermi level. As a consequence of this approximation, the 1p-1h and 2p-2h states have good isospin too.

4.2. THE RESIDUAL INTERACTION

We have taken the simplest effective interaction which has been shown [16]) to give satisfying results in the 1p-1h description of ^{40}Ca:

$$v(i, j) = -V_0 \delta(r_i - r_j)(\Pi_t + p\Pi_s), \tag{4.1a}$$

where Π_t and Π_s project on triplet and singlet spin states respectively. The values of the parameters are:

$$V_0 = 986 \text{ MeV} \cdot \text{fm}^3, \quad p = 0.46. \tag{4.1b}$$

However, calculations of the effective interaction based on the Brueckner theory show that the effective interaction should be density dependent [17]). Therefore, we also

consider the two following interactions:

$$\text{(F1)}\ v(\boldsymbol{R}, \boldsymbol{r}) = -1160\ \text{MeV}\cdot\text{fm}^3[1-0.845\ \text{fm}^2\rho^{\frac{2}{3}}(\boldsymbol{R})]\delta(\boldsymbol{r}). \tag{4.2}$$

$$\text{(F2)}\ v(\boldsymbol{R}, \boldsymbol{r}) = -538.3\ \text{MeV}\cdot\text{fm}^3[1+0.0385\ \text{fm}^2\rho^{\frac{2}{3}}(\boldsymbol{R})+0.147\ \text{fm}^{-1}\rho^{-\frac{1}{3}}(\boldsymbol{R})]\delta(\boldsymbol{r}), \tag{4.3}$$

where $\boldsymbol{R}$ and $\boldsymbol{r}$ denote the c.m. coordinate and the relative coordinate of the two nucleons, respectively. The interaction F1 has been obtained from the modified delta interaction of Moszkowski [18]) by suppressing the velocity-dependent term. The latter simulates a hard core and ensures saturation, but is not important in the excitation of particle-hole pairs. The interaction F2 is derived from the interaction used by Lassey and Volkov [19]), in the same manner. These two interactions present, however, the drawback of being as strong in the singlet state as in the triplet state. The importance of the density-dependence will be hard to visualize in a comparison with the results given by (4.1). For this reason, we have examined interactions F3 and F4 which have the same density dependence of the forces F1 and F2, the same triplet-singlet ratio as the interaction (4.1) and an intensity such that they are equal to (4.1) in the nuclear interior. We can give F1–F4 the form:

$$v(\boldsymbol{R}, \boldsymbol{r}) = -V_0(\Pi_t + p\Pi_s)\xi(\eta, \zeta, \rho(\boldsymbol{R}))\delta(\boldsymbol{r}), \tag{4.4a}$$

with

$$\xi(\eta, \zeta, \rho(\boldsymbol{R})) = 1+\eta\rho^{\frac{2}{3}}(\boldsymbol{R})+\zeta\rho^{-\frac{1}{3}}(\boldsymbol{R}). \tag{4.4b}$$

The values of the parameters are:

$$\text{F1:}\ V_0 = 1160\ \text{MeV}\cdot\text{fm}^3,\ p = 1,\ \eta = -0.845\ \text{fm}^2,\ \zeta = 0, \tag{4.4c}$$

$$\text{F2:}\ V_0 = 538.3\ \text{MeV}\cdot\text{fm}^3,\ p = 1,\ \eta = 0.0385\ \text{fm}^2,\ \zeta = 0.147\ \text{fm}^{-1}, \tag{4.4d}$$

$$\text{F3:}\ V_0 = 1290\ \text{MeV}\cdot\text{fm}^3,\ p = 0.46,\ \eta = -0.845\ \text{fm}^2,\ \zeta = 0, \tag{4.4e}$$

$$\text{F4:}\ V_0 = 713\ \text{MeV}\cdot\text{fm}^3,\ p = 0.46,\ \eta = 0.0385\ \text{fm}^2,\ \zeta = 0.147\ \text{fm}^{-1}. \tag{4.4f}$$

In the following, we focus our attention on the calculation with interaction (4.1), mentioning only the important differences introduced by the density dependence.

4.3. THE FORM FACTORS

With the help of eqs. (3.1) and (2.12) and the remark at the end of sect. 3, we can write:

$$\mathscr{V}_E^{\text{opt}(c)}(E', E'') = v_0+\mathscr{V}^{\text{CN}}(E', E'')+\mathscr{V}^{\text{DIR}}(E', E''), \tag{4.5a}$$

with

$$\mathscr{V}^{\text{CN}}(E', E'') = \sum_s \langle\chi^c_{E'}|V|\phi_s\rangle(E+iI_{\text{eff}}-E_s)^{-1}\langle\phi_s|V|\chi^c_{E''}\rangle + \sum_l \langle\chi^c_{E'}|V|\phi_l\rangle(E+iI-E_l)^{-1}\langle\phi_l|V|\chi^c_{E''}\rangle, \tag{4.5b}$$

$$\mathscr{V}^{\text{DIR}}(E', E'') = -i\pi\sum_{c'\neq c}\langle\chi^c_{E'}|V|\chi^{c'}_E\rangle\langle\chi^{c'}_E|V|\chi^c_{E''}\rangle. \tag{4.5c}$$

TABLE 2

Proton elastic channels for $l \leqq 4$

J^π	Particle	Number		J^π	Particle	Number	
		$T=1$	$T=0$			$T=1$	$T=0$
0^+	$d_{\frac{3}{2}}$	1	24	2^-	$p_{\frac{1}{2}}$	13	36
0^-	$p_{\frac{3}{2}}$	2	25		$p_{\frac{3}{2}}$	14	37
1^+	$s_{\frac{1}{2}}$	3	26		$f_{\frac{5}{2}}$	15	38
	$d_{\frac{3}{2}}$	4	27		$f_{\frac{7}{2}}$	16	39
	$d_{\frac{5}{2}}$	5	28	3^+	$d_{\frac{3}{2}}$	17	40
1^-	$p_{\frac{1}{2}}$	6	29		$d_{\frac{5}{2}}$	18	41
	$p_{\frac{3}{2}}$	7	30		$g_{\frac{7}{2}}$	19	42
	$f_{\frac{7}{2}}$	8	31		$g_{\frac{9}{2}}$	20	43
2^+	$s_{\frac{1}{2}}$	9	32	3^-	$p_{\frac{3}{2}}$	21	44
	$d_{\frac{3}{2}}$	10	33		$f_{\frac{5}{2}}$	22	45
	$d_{\frac{5}{2}}$	11	34		$f_{\frac{7}{2}}$	23	46
	$g_{\frac{7}{2}}$	12	35				

The hole is $1d_{\frac{3}{2}}$. $\varepsilon_c = 10.0872$ MeV.

TABLE 3

One-particle-one-hole compound states

No.	J^π	Particle-hole	Type	Energy	No.	J^π	Particle-hole	Type	Energy
1	0^+	$(2p_{\frac{3}{2}})_n(1p_{\frac{1}{2}})_n^{-1}$	1	22.52	22		$(1f_{\frac{7}{2}})_n(1p_{\frac{1}{2}})_n^{-1}$	3	16.33
2		$(2p_{\frac{3}{2}})_n(1p_{\frac{3}{2}})_n^{-1}$	1	22.75	23		$(1f_{\frac{7}{2}})_n(1p_{\frac{3}{2}})_n^{-1}$	3	18.78
3	0^-	$(2p_{\frac{1}{2}})_n(2s_{\frac{1}{2}})_n^{-1}$	2	12.66	24	3^-	$(2p_{\frac{1}{2}})_n(1d_{\frac{5}{2}})_n^{-1}$	1	15.78
4	1^+	$(2p_{\frac{3}{2}})_n(1p_{\frac{1}{2}})_n^{-1}$	1	22.52	25		$(2p_{\frac{3}{2}})_n(1d_{\frac{3}{2}})_n^{-1}$	1	13.76
5		$(2p_{\frac{1}{2}})_n(1p_{\frac{3}{2}})_n^{-1}$	1	24.97	26		$(1f_{\frac{7}{2}})_n(1s_{\frac{1}{2}})_n^{-1}$	3	27.31
6		$(2p_{\frac{3}{2}})_n(1p_{\frac{1}{2}})_n^{-1}$	1	20.50	27	0^+	$(2p_{\frac{3}{2}})_p(1p_{\frac{3}{2}})_p^{-1}$	1	23.55
7		$(2p_{\frac{3}{2}})_n(1p_{\frac{3}{2}})_n^{-1}$	1	22.75	28	1^-	$(2p_{\frac{3}{2}})_p(1p_{\frac{3}{2}})_p^{-1}$	1	23.55
8	1^-	$(2p_{\frac{3}{2}})_n(1d_{\frac{5}{2}})_n^{-1}$	1	13.56	29		$(2p_{\frac{3}{2}})_p(1p_{\frac{1}{2}})_p^{-1}$	1	21.11
9		$(2p_{\frac{1}{2}})_n(1s_{\frac{1}{2}})_n^{-1}$	1	34.50	30		$(2p_{\frac{3}{2}})_p(1d_{\frac{5}{2}})_p^{-1}$	1	14.24
10		$(2p_{\frac{3}{2}})_n(1s_{\frac{1}{2}})_n^{-1}$	1	31.28	31		$(2p_{\frac{3}{2}})_p(1s_{\frac{1}{2}})_p^{-1}$	1	32.04
11		$(2p_{\frac{1}{2}})_n(2s_{\frac{1}{2}})_n^{-1}$	2	12.66	32	2^+	$(2p_{\frac{3}{2}})_p(1p_{\frac{1}{2}})_p^{-1}$	1	21.11
12		$(2p_{\frac{1}{2}})_n(1d_{\frac{3}{2}})_n^{-1}$	1	11.59	33		$(2p_{\frac{3}{2}})_p(1p_{\frac{3}{2}})_p^{-1}$	1	23.55
13	2^+	$(2p_{\frac{3}{2}})_n(1p_{\frac{1}{2}})_n^{-1}$	1	20.50	34		$(1f_{\frac{7}{2}})_p(1p_{\frac{3}{2}})_p^{-1}$	3	19.13
14		$(2p_{\frac{1}{2}})_n(1p_{\frac{3}{2}})_n^{-1}$	1	24.97	35	2^-	$(2p_{\frac{3}{2}})_p(1d_{\frac{5}{2}})_p^{-1}$	1	14.24
15		$(2p_{\frac{3}{2}})_n(1p_{\frac{3}{2}})_n^{-1}$	1	22.75	36		$(2p_{\frac{3}{2}})_p(1s_{\frac{1}{2}})_p^{-1}$	1	32.04
16		$(1f_{\frac{7}{2}})_n(1p_{\frac{3}{2}})_n^{-1}$	3	18.78	37	3^+	$(2p_{\frac{3}{2}})_p(1p_{\frac{3}{2}})_p^{-1}$	1	23.55
17	2^-	$(2p_{\frac{1}{2}})_n(1d_{\frac{5}{2}})_n^{-1}$	1	15.78	38		$(1f_{\frac{7}{2}})_p(1p_{\frac{1}{2}})_p^{-1}$	3	17.69
18		$(2p_{\frac{3}{2}})_n(1d_{\frac{5}{2}})_n^{-1}$	1	13.56	39		$(1f_{\frac{7}{2}})_p(1p_{\frac{3}{2}})_p^{-1}$	3	19.13
19		$(2p_{\frac{3}{2}})_n(1s_{\frac{1}{2}})_n^{-1}$	1	31.28	40	3^-	$(2p_{\frac{3}{2}})_p(1d_{\frac{5}{2}})_p^{-1}$	1	14.24
20		$(2p_{\frac{1}{2}})_n(1d_{\frac{3}{2}})_n^{-1}$	1	11.49	41		$(1f_{\frac{7}{2}})_p(1s_{\frac{1}{2}})_p^{-1}$	3	27.62
21	3^+	$(2p_{\frac{1}{2}})_n(1p_{\frac{3}{2}})_n^{-1}$	1	22.75					

The type of the state is 1, (2, 3) if its form factor is approximated by g, (h, k) (see eq. (4.12)).
Nos. 1–41: $T = 1$. Nos. 42–82: $T = 0$.

TABLE 4

Inelastic channels corresponding to 1p-1h states

J^π	Configuration	Number				Type	$P_{c'}$
		$T=1$		$T=0$			
		neutron	proton	neutron	proton		
0^+	$s_{\frac{1}{2}}(2s_{\frac{1}{2}})^{-1}$	1	35	69	103	2	0.125
	$d_{\frac{5}{2}}(1d_{\frac{5}{2}})^{-1}$	2	36	70	104	1	0.300
0^-	$p_{\frac{1}{2}}(1s_{\frac{1}{2}})^{-1}$	3	37	71	105	2	0.200
	$f_{\frac{5}{2}}(1d_{\frac{5}{2}})^{-1}$	4	38	72	106	3	0.125
1^+	$s_{\frac{1}{2}}(2s_{\frac{1}{2}})^{-1}$	5	38	73	107	2	0.125
	$d_{\frac{3}{2}}(2s_{\frac{1}{2}})^{-1}$	6	40	74	108	2	0.125
	$d_{\frac{3}{2}}(1d_{\frac{5}{2}})^{-1}$	7	41	75	109	1	0.250
	$d_{\frac{5}{2}}(1d_{\frac{5}{2}})^{-1}$	8	42	76	110	1	0.300
1^-	$p_{\frac{1}{2}}(2s_{\frac{1}{2}})^{-1}$	9	43	77	111	2	0.200
	$p_{\frac{3}{2}}(2s_{\frac{1}{2}})^{-1}$	10	44	78	112	2	0.200
	$p_{\frac{3}{2}}(1d_{\frac{5}{2}})^{-1}$	11	45	79	113	1	0.100
	$f_{\frac{5}{2}}(1d_{\frac{5}{2}})^{-1}$	12	46	80	114	3	0.100
	$f_{\frac{7}{2}}(1d_{\frac{5}{2}})^{-1}$	13	47	81	115	3	0.100
2^+	$d_{\frac{3}{2}}(2s_{\frac{1}{2}})^{-1}$	14	48	82	116	2	0.200
	$d_{\frac{5}{2}}(2s_{\frac{1}{2}})^{-1}$	15	49	83	117	2	0.200
	$s_{\frac{1}{2}}(1d_{\frac{5}{2}})^{-1}$	16	50	84	118	3	0.250
	$d_{\frac{3}{2}}(1d_{\frac{5}{2}})^{-1}$	17	51	85	119	1	0.250
	$d_{\frac{5}{2}}(1d_{\frac{5}{2}})^{-1}$	18	52	86	120	1	0.300
2^-	$p_{\frac{3}{2}}(2s_{\frac{1}{2}})^{-1}$	19	53	87	121	2	0.200
	$f_{\frac{5}{2}}(2s_{\frac{1}{2}})^{-1}$	20	54	88	122	1	0.100
	$p_{\frac{1}{2}}(1d_{\frac{5}{2}})^{-1}$	21	55	89	123	1	0.100
	$p_{\frac{3}{2}}(1d_{\frac{5}{2}})^{-1}$	22	56	90	124	1	0.100
	$f_{\frac{5}{2}}(1d_{\frac{5}{2}})^{-1}$	23	57	91	125	3	0.100
	$f_{\frac{7}{2}}(1d_{\frac{5}{2}})^{-1}$	24	58	92	126	3	0.100
3^+	$d_{\frac{5}{2}}(2s_{\frac{1}{2}})^{-1}$	25	59	93	127	2	0.200
	$s_{\frac{1}{2}}(1d_{\frac{5}{2}})^{-1}$	26	60	94	128	3	0.250
	$d_{\frac{3}{2}}(1d_{\frac{5}{2}})^{-1}$	27	61	95	129	1	0.300
	$d_{\frac{5}{2}}(1d_{\frac{5}{2}})^{-1}$	28	62	96	130	1	0.300
3^-	$f_{\frac{5}{2}}(2s_{\frac{1}{2}})^{-1}$	29	63	97	131	1	0.100
	$f_{\frac{7}{2}}(2s_{\frac{1}{2}})^{-1}$	30	64	98	132	1	0.100
	$p_{\frac{1}{2}}(1d_{\frac{5}{2}})^{-1}$	31	65	99	133	1	0.100
	$p_{\frac{3}{2}}(1d_{\frac{5}{2}})^{-1}$	32	66	100	134	1	0.100
	$f_{\frac{5}{2}}(1d_{\frac{5}{2}})^{-1}$	33	67	101	135	3	0.120
	$f_{\frac{7}{2}}(1d_{\frac{5}{2}})^{-1}$	34	68	102	136	3	0.120
0^+	$d_{\frac{3}{2}}(1d_{\frac{3}{2}})^{-1}$	137		144		1	0.300
0^-	$p_{\frac{3}{2}}(1d_{\frac{3}{2}})^{-1}$	138		145		1	0.100
1^+	$d_{\frac{3}{2}}(1d_{\frac{3}{2}})^{-1}$	139		146		1	0.250
	$s_{\frac{1}{2}}(1d_{\frac{3}{2}})^{-1}$	140		147		3	0.250
	$f_{\frac{5}{2}}(1d_{\frac{3}{2}})^{-1}$	141		148		3	0.100
1^-	$p_{\frac{1}{2}}(1d_{\frac{3}{2}})^{-1}$	142		149		1	0.100
	$p_{\frac{1}{2}}(1d_{\frac{3}{2}})^{-1}$	143		150		3	0.100

The meaning of the coefficient $P_{c'}$ is explained in the text.

Contact interactions like those of subsect. 4.2 yield a simple expression for the form factors. Indeed, we have then for the interaction (4.1), since χ_E^c and ϕ_s are 1p-1h states [20]):

$$\langle \chi_{E'}^c | V | \phi_s \rangle = f_s^c I_s^c(E'), \tag{4.6a}$$

$$\langle \chi_{E'}^c | V | \chi_E^{c'} \rangle = f^{cc'} I_{cc'}(E', E), \tag{4.6b}$$

with

$$I_s^c(E') = \int_0^\infty w_{p_s}(r) w_{h_s}(r) w_{h_c}(r) u_c(r, k_c') r^{-2} \mathrm{d}r, \tag{4.7}$$

$$I_{cc'}(E', E) = \int_0^\infty w_{h_c}(r) w_{h_{c'}}(r) u_c(r, k_c') u_{c'}(r, k_{c'}) r^{-2} \mathrm{d}r. \tag{4.8}$$

The functions w are the single-particle wave functions for bound orbitals and the functions u_c correspond to scattering orbitals. The quantities k_c' are related to E' by the relation (2.3). The coefficients f_s^c and $f^{cc'}$ only depend upon the quantum numbers of the states $\chi_{E'}^c$ and ϕ_s (or $\chi_{E'}^c$ and $\chi_E^{c'}$), and upon the parameters V_0 and p of the interaction (4.1). Their explicit expressions can be found in ref. [20]). For the matrix element $\langle \chi_{E'}^c | V | \phi_l \rangle$, a relation similar to (4.6a) holds, but the coefficients f_l^c are much more complicated.

Let us now write eq. (4.5) in the r-representation, using relation (2.12d). Because of the closure relation for the single-particle states in potential v_0, we have:

$$\langle \chi_r^c | V | \phi_s \rangle = f_s^c I_s^c(r) - \sum_n w_{l_j}(r, k_n) \int_0^\infty \mathrm{d}r' w_{l_j}(r', k_n) I_s^c(r'), \tag{4.9}$$

with

$$I_s^c(r) = w_{p_s}(r) w_{h_s}(r) w_{h_c}(r) r^{-2}, \tag{4.10}$$

and a similar relation for $\langle \chi_{E'}^c | V | \chi_E^{c'} \rangle$. The second term in the r.h.s. of relation (4.9) does not act on the OM wave function as defined in eq. (2.4). We can thus drop this term, and get:

$$\mathscr{V}^{\mathrm{CN}}(r, r') = \sum_s \frac{(f_s^c)^2}{E - E_s + iI_{\mathrm{eff}}} I_s^c(r) I_s^c(r') + \sum_l \frac{(f_l^c)^2}{E - E_l + iI} I_l^c(r) I_l^c(r'), \tag{4.11a}$$

$$\mathscr{V}^{\mathrm{DIR}}(r, r') = -i\pi \sum_{c' \neq c} (f^{cc'})^2 I_{cc'}(r) I_{cc'}(r'). \tag{4.11b}$$

In table 2, we quote the 1p-1h elastic channels up to $l = 4$ (the classical limit corresponds to $l_{cl} \approx 3$ at the energy considered). In tables 3 and 4, we quote the 1p-1h compound nucleus states of ^{40}Ca up to 35 MeV above the ground state (of spin $J \leqq 3$) and the inelastic channels open at the energy considered (i.e. 24 MeV above the ground state). We compute all the quantities $I_s^c(r)$. They can be approximated to a good accuracy by one of the three functions

$$\begin{Bmatrix} g(r) \\ h(r) \\ k(r) \end{Bmatrix} = c \left[\exp\left\{ -\left(\frac{r - r_{0s}}{a_s} \right)^2 \right\} + \begin{Bmatrix} +1 \\ -1 \\ 0 \end{Bmatrix} z \exp\left\{ -\left(\frac{r - x r_{0s}}{y a_s} \right)^2 \right\} \right], \tag{4.12}$$

with $c = 0.02\ \text{fm}^{-\frac{7}{2}}$, $r_{0s} = 2.2$ fm, $a_s = 0.6$ fm, $x = 1.8$, $y = 0.6$, $z = 0.5$. The quantities $I_{cc'}(r)$ could also be approximated by the same functions times a constant factor $P_{c'}$ which depends upon the channel c' and which reflects the penetration of a scattering wave in this channel. The degree of accuracy is depicted by fig. 1, which shows the shape of some form factors. These approximations can be done because of the

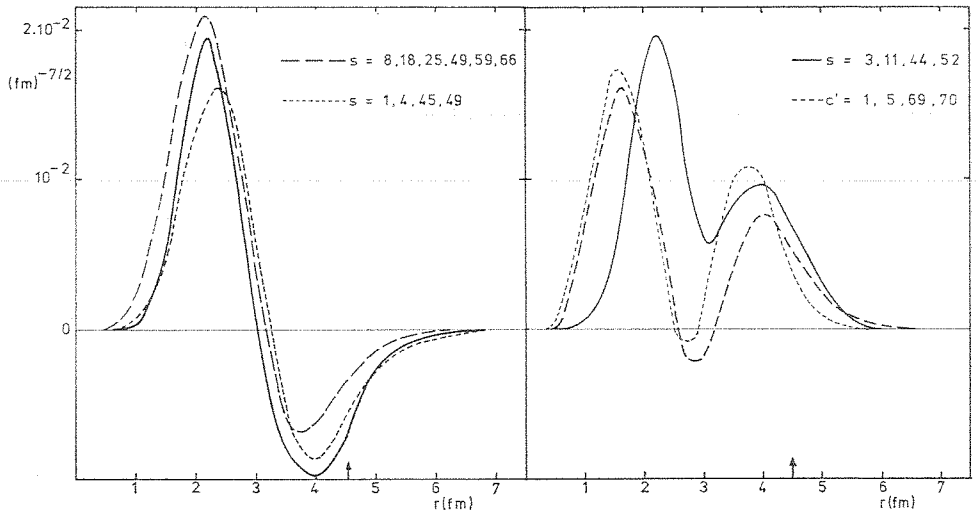

Fig. 1. Comparison of form factors from some states ϕ_s and $\chi_E^{c'}$ with the functions $g(r)$ (left) and $h(r)$ (right), which are represented by full lines.

rather weak excitation energy considered. Then, the orbitals coming into eq. (4.10) are those of a few single-particle states around the Fermi level. The different combinations are not very numerous. We can now, gathering the results (4.11), (2.14) and (2.15), write the OMP for a given partial wave L as:

$$\mathscr{V}_L^{\text{opt}} = v_0 + \overline{\mathscr{V}}_L(r, r') = v_0 + \mathscr{V}_L^{\text{CN}}(r, r') + \mathscr{V}_L^{\text{DIR}}(r, r'), \tag{4.13a}$$

with

$$\mathscr{V}_L^{\text{CN}}(r, r') = \sum_j (L0\tfrac{1}{2}\tfrac{1}{2}|j\tfrac{1}{2})^2 (2I_c+1)^{-1} \sum_{\mu_I} \sum_J (j\tfrac{1}{2} I_c \mu_I | J\mu_I + \tfrac{1}{2})^2$$

$$\times \sum_T (T_c M_{T_c} t m_t | T M_T)^2 \sum_{c=LjJT} \left\{ \left[\sum_{[s_1]} \frac{(f_{s_1}^c)^2}{E + iI_{\text{eff}} - E_{s_1}} + \sum_{[l_1]} \frac{(f_{l_1}^c)^2}{E - E_{l_1} + iI} \right] \right.$$

$$\times g(r)g(r') + \left[\sum_{[s_2]} \frac{(f_{s_2}^c)^2}{E - E_{s_2} + iI_{\text{eff}}} + \sum_{[l_2]} \frac{(f_{l_2}^c)^2}{E - E_{l_2} + iI} \right] h(r)h(r')$$

$$\left. + \left[\sum_{[s_3]} \frac{(f_{s_3}^c)^2}{E - E_{s_3} + iI_{\text{eff}}} + \sum_{[l_3]} \frac{(f_{l_3}^c)^2}{E - E_{l_3} + iI} \right] k(r)k(r') \right\}, \tag{4.13b}$$

$$\mathscr{V}_L^{\mathrm{DIR}}(r,r') = \sum_j (L0\tfrac{1}{2}\tfrac{1}{2}|j\tfrac{1}{2})^2(2I_c+1)^{-1}\sum_{\mu_I}\sum_J (j\tfrac{1}{2}I_c\mu_I|J\mu_I+\tfrac{1}{2})^2$$
$$\times \sum_T (T_c M_{T_c} tm_t|TM_T)^2 \sum_{c=LjJT}\{-i\pi[\sum_{[c'_1]\neq c}(f^{cc'_1}P_{c'_1})^2 g(r)g(r')$$
$$+\sum_{[c'_2]\neq c}(f^{cc'_2}P_{c'_2})^2 h(r)h(r')+\sum_{[c'_3]\neq c}(f^{cc'_3}P_{c'_3})^2 k(r)k(r')]\}. \qquad (4.13c)$$

The indices $[s_1]$, $[l_1]$, $[c'_1]$ denote that the sum is restricted to the states with the same quantum numbers as those of channel c such that the quantities $I^c_{s_1}$, $I^c_{l_1}$, and $I_{cc'_1}$ can be approximated by the function $g(r)$. The same convention holds for $[s_2]$, $[l_2]$, $[c'_2]$ in relation to $h(r)$, and $[s_3]$, $[l_3]$, $[c'_3]$ in relation to $k(r)$. Eq. (4.13b) and (4.13c) can also be written as

$$\begin{Bmatrix}\mathscr{V}_L^{\mathrm{CN}}\\ \mathscr{V}_L^{\mathrm{DIR}}\end{Bmatrix} = (X_g+iW_g)g(r)g(r')+(X_h+iW_h)h(r)h(r')+(X_k+iW_k)k(r)k(r') \qquad (4.14)$$

with obvious notation. Of course, the X-coefficients are equal to zero for $\mathscr{V}_L^{\mathrm{DIR}}$.

TABLE 5

Coefficients X and W (MeV · fm^6) for the compound-states contribution (see eq. (4.14))

	$l=0$		$l=1$		$l=2$		$l=3$	
	X_α	W_α	X_α	W_α	X_α	W_α	X_α	W_α
1p-1h contribution:								
$\alpha=g$	−1202	−2888	531	−434	930	−2613	353	−294
$\alpha=h$	0	0	12	− 3	0	0	0	0
$\alpha=k$	1854	−1103	−696	−606	543	− 314	−281	245
2p-2h contribution:								
$\alpha=g$	115	− 94	−142	− 35	85	− 69	− 63	− 15
$\alpha=h$	115	− 314	− 94	− 10	85	− 239	− 43	− 4
$\alpha=k$	31	0	18	−168	22	− 2	8	− 75
total contribution:								
$\alpha=g$	−1087	−2984	−389	−469	1015	−2682	290	−308
$\alpha=h$	115	− 314	− 82	− 13	85	− 238	− 43	− 4
$\alpha=k$	1885	−1103	−678	−774	565	− 316	−273	−320

4.4. COMPOUND NUCLEUS CONTRIBUTION

In order to compute the quantities X_g and W_g corresponding to $\mathscr{V}_L^{\mathrm{CN}}$, we must choose the values of I and I_{eff}. The interval I must reflect the experimental situation, and a value of 1 MeV seems reasonable. The quantity I_{eff} depends upon the spreading width of the 1p-1h states, whose computation is very complicated. There exist in the literature [21,22]) some estimates, which indicate that $I_{\mathrm{eff}} = 3$ MeV is a reasonable value. We have avoided the computation of the coefficients f^c_l by taking $(f^c_l)^2 \approx \overline{(f^c_s)^2}^s$. This is probably an overestimate. Indeed, one can expect that the angular

overlap between two 1p-1h states (χ_E^c and ϕ_s) is more important than that between a 1p-1h state and a 2p-2h state (χ_E^c and ϕ_l).

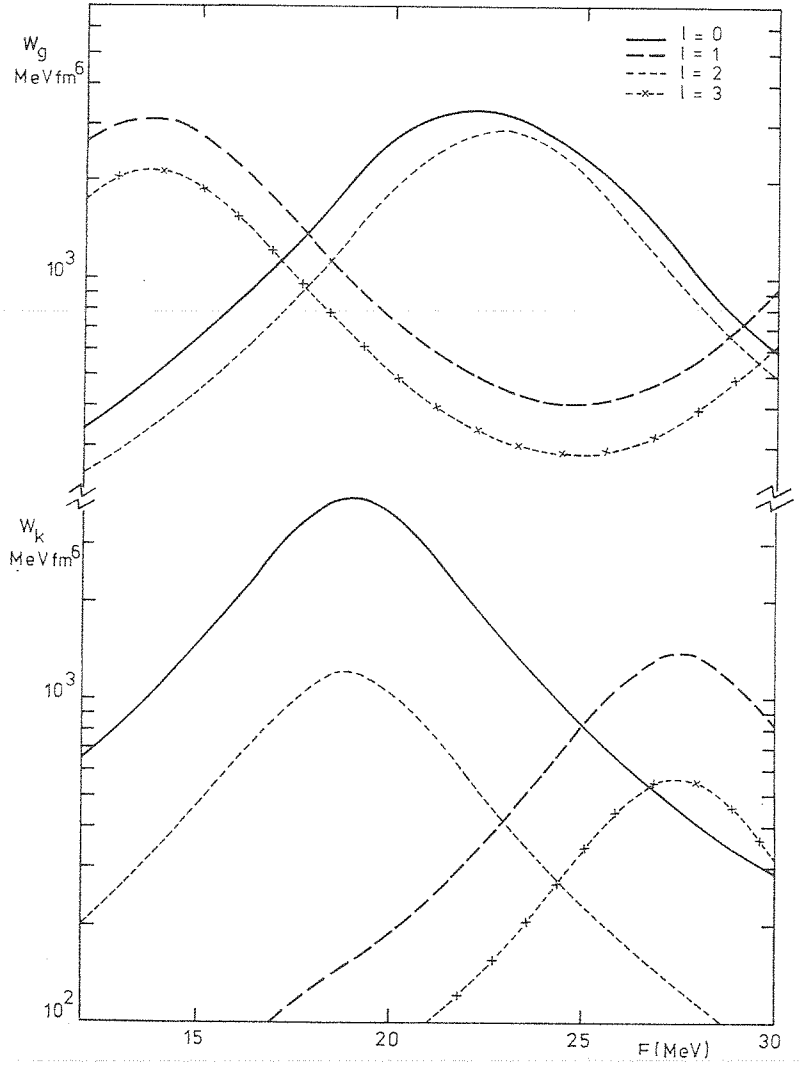

Fig. 2. Dependence of the coefficients W_g and W_k for the compound-states contribution (see eq. (4.14)) upon excitation energy. The origin is the ^{40}Ca ground state energy.

The coefficients X and W computed along these lines are quoted in table 5. One sees that the contribution of the 2p-2h states (apart from I_{eff}) directly coupled to the incident channels is very small compared to the contribution of the 1p-1h states. The reason is their small density in the energy region of interest (24 MeV above the ground state, 14 MeV above the proton emission threshold). The quantities X are in general

smaller than the corresponding quantities W, but sometimes of the same magnitude (for $L = 1$ and $L = 3$). Their sign fluctuates while the sign of W is always negative. The quantities W are always smaller for $L = 1$ and $L = 3$ than for $L = 0$ and $L = 2$. This is due to the grouping of the states ϕ_s according to their parity. From 10 to 17

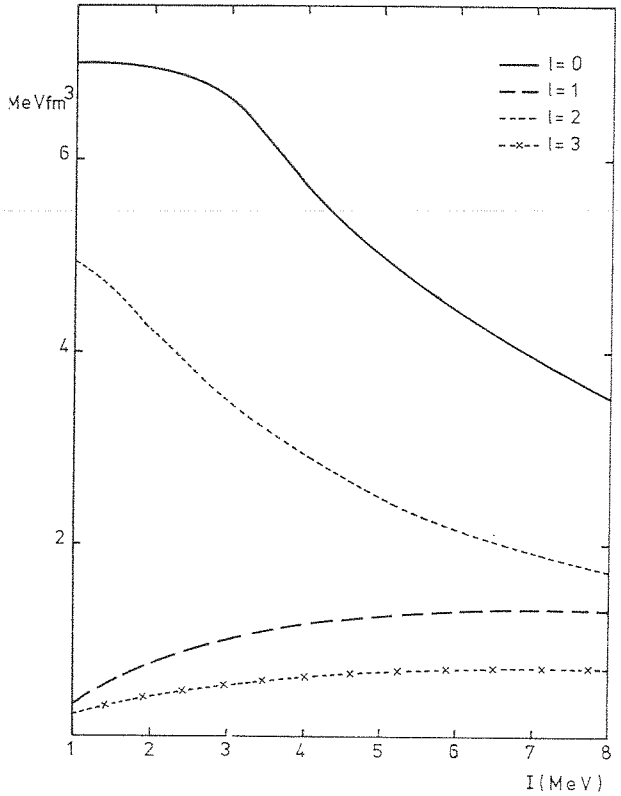

Fig. 3. Plot of the compound-states contribution [eq. (4.13b) integrated over radial variables] versus the averaging interval. The excitation energy is 24 MeV above the ^{40}Ca ground state.

MeV and from 27 to 34 MeV, most of the states have negative parity. From 17 to 25 MeV, the parity is generally positive. Accordingly, the absorption at 24 MeV mainly takes place in the positive-parity channels, which corresponds to $L = 0$ and $L = 2$ incident protons (the spin and parity of ^{39}K are $\frac{3}{2}^+$). This is confirmed by fig. 2 which shows the variation of W_g and W_k with excitation energy. This is also illustrated by fig. 3, which exhibits the variation of the radial integral of Im $\mathscr{V}_L^{\mathrm{CN}}$ with respect to I_{eff} at $E = 24$ MeV. Indeed, for the $L = 1$ and $L = 3$ partial waves, what mainly contribute to Im $\mathscr{V}_L^{\mathrm{CN}}$ are the far-lying states, i.e. those for which $|E-E_s| > I_{\mathrm{eff}}$ [see eq. (4.13b)]. Therefore, the imaginary part increases with I_{eff}. On the other hand, the contribution to Im $\mathscr{V}_L^{\mathrm{CN}}$ for the $L = 0$ and $L = 2$ partial waves, comes from the

nearby states for which $|E-E_s| \lesssim I_{\text{eff}}$. If I_{eff} increases, their contribution decreases as I_{eff}^{-1} for large values of I_{eff}. The channels $L = 4$ are weakly absorbed because of the weak coupling to the states ϕ_s.

4.5. DIRECT INTERACTION CONTRIBUTION

Here, we discuss the contribution which comes from the excitation of the inelastic channels. The values of the coefficients W corresponding to the quantities $\mathscr{V}_L^{\text{DIR}}$ are given in table 6, as well as the coefficients W corresponding to the summation of $\mathscr{V}_L^{\text{CN}}$ and $\mathscr{V}_L^{\text{DIR}}$. Again, the $L = 0$ and $L = 2$ partial waves are more absorbed than the odd

TABLE 6

Coefficients W (MeV · fm^6) for the inelastic-channels contribution and total contribution (see eq. (4.14))

	$L=0$	$L=1$	$L=2$	$L=3$	$L=4$
Inelastic:					
W_g	−2473	− 214	−3470	−151	−422
W_h	−1442	− 546	− 539	−353	−177
W_k	−1209	− 533	− 388	−268	−267
Total:					
W_g^L	−5757	− 684	−6152	−459	−422
W_h^L	−1756	− 560	− 777	−356	−177
W_k^L	−2312	−1307	− 704	−588	−267

partial waves. One can see from tables 5 and 6 that the contribution of the compound nucleus states and that of the inelastic channels are comparable. If one computes the volume integral of the imaginary part of the OMP, one gets $\mathscr{J}_V = -158$ MeV · fm^3, decomposing into -68 MeV · fm^3 for the compound-states contribution and -90 MeV · fm^3 for the inelastic-channels contribution.

5. Equivalent local potential: comparison with experiment

It is not easy to visualize non-local potentials, nor to compute the cross sections derived from them for direct comparison with experimental data. We first try to build an equivalent local potential (ELP), which gives the same phase shifts as the non-local potential we have constructed. Afterwards, we compute cross sections from this ELP and compare them with experiment.

5.1. EQUIVALENT LOCAL POTENTIAL

We assume, in the following, that the real part of the OMP is given by v_0. The OMP for a given partial wave L can then be written:

$$\mathscr{V}_L^{\text{opt}} = v_0 + iW_g^L g(r)g(r') + iW_h^L h(r)h(r') + iW_k^L k(r)k(r'), \qquad (5.1)$$

where the W are those of the second part of table 6. In this subsection, we attempt to construct an ELP of (5.1) in two steps: (i) We find an ELP of $v_0(r)+iW_g^L g(r)g(r')$. Fiedeldey [23]) has described a method for constructing an ELP of a non-local potential. We generalize this method to the case where the potential has both a local part and a non-local separable one. (ii) We compute the ELP of the potential (5.1) following the scheme:

$$\mathrm{ELP}\,\{\mathrm{ELP}\,[\mathrm{ELP}\,(v_0+iW_g^L g(r)g(r'))+iW_h^L h(r)h(r')]+iW_k^L k(r)k(r')\}. \tag{5.2}$$

We show that it is a good approximation.

We start from the radial Schrödinger equation:

$$\left[\frac{\mathrm{d}^2}{\mathrm{d}r^2}-\frac{l(l+1)}{r^2}-\frac{2m}{\hbar^2}v_0(r)+k^2\right]u(r)=W_0\,g(r)\int g(r')u(r')\,\mathrm{d}r', \tag{5.3}$$

where W_0 reduces to $i(2m/\hbar^2)W_g^L$, while $u(r)$ is the regular solution at the origin. Let $\psi(r)$ be the regular solution of the local equation. We write:

$$u(r)=F(r)\psi(r), \tag{5.4}$$

$$\left[\frac{\mathrm{d}^2}{\mathrm{d}r^2}-\frac{l(l+1)}{r^2}-\frac{2m}{\hbar^2}(v_0(r)+U(r))+k^2\right]\psi(r)=0. \tag{5.5}$$

The quantity $F(r)$ is the "damping" factor. It is easy to verify that the following result, obtained by Coz *et al.* [24]) for a separable potential, remains valid if one adds a local part

$$U(r)=-\frac{1}{2}\frac{W''(r)}{W(r)}+\frac{3}{4}\frac{W'(r)}{W(r)}-\frac{g(r)}{W(r)}\frac{\mathrm{d}}{\mathrm{d}r}\left(\frac{W'(r)}{g(r)}\right), \tag{5.6}$$

where the "non-local Wronskian" $W(r)$ is given by:

$$W(r)=k^{-1}\{u'(r)v(r)-u(r)v'(r)\}. \tag{5.7}$$

The function v is the irregular solution of eq. (5.3). The functions u and v behave asymptotically like:

$$\begin{Bmatrix}u\\v\end{Bmatrix}\underset{r\to\infty}{\sim}\begin{Bmatrix}\sin\\\cos\end{Bmatrix}(kr+\delta_l-\tfrac{1}{2}l\pi-\gamma\ln(lkr)+\sigma_l). \tag{5.8}$$

The quantity $W(r)$ is related to the damping factor by the relation

$$F^2(r)=W(r)[W(\infty)]^{-1}. \tag{5.9}$$

In order to obtain the expression for the non-local Wronskian, we start from the integral form of u and v [ref. [25])]:

$$\begin{Bmatrix}u(r)\\v(r)\end{Bmatrix}=\begin{Bmatrix}\mathscr{J}(r)\\\mathscr{N}(r)\end{Bmatrix}-\frac{W_0}{k}\int_0^r g(r')H(r,r')\,\mathrm{d}r'\int_0^\infty g(s)\begin{Bmatrix}u(s)\\v(s)\end{Bmatrix}\mathrm{d}s, \tag{5.10}$$

$\mathscr{J}$ and $\mathscr{N}$ being the regular and irregular solutions for the potential v_0 alone, which behave asymptotically as u and v, except for the phase shift. The Green function is given by:

$$H(r, r') = \mathscr{J}(r')\mathscr{N}(r) - \mathscr{J}(r)\mathscr{N}(r'). \tag{5.11}$$

The derivatives of u and v are equal to

$$\begin{Bmatrix} u'(r) \\ v'(r) \end{Bmatrix} = \begin{Bmatrix} \mathscr{J}'(r) \\ \mathscr{N}'(r) \end{Bmatrix} - \frac{W_0}{k} \int_0^r g(r') \frac{\partial H(r, r')}{\partial r} \, dr' \int_0^\infty g(s) \begin{Bmatrix} u(s) \\ v(s) \end{Bmatrix} ds, \tag{5.12}$$

since $H(r, r) = 0$. In eq. (5.10) and (5.12), one can replace the functions u and v in the integrals by $\mathscr{J}$ and $\mathscr{N}$ respectively, provided they are multiplied by a factor α, which can be calculated by multiplying eq. (5.10) by $g(r)$ and integrating over r. This factor is

$$\alpha^{-1} = 1 - \frac{W_0}{k} \left\{ \int_0^\infty g(s)\mathscr{N}(s) ds \int_0^s g(t)\mathscr{J}(t) dt - \int_0^\infty ds\, g(s)\mathscr{J}(s) \int_0^s g(t)\mathscr{N}(t) dr \right\}. \tag{5.13}$$

We also find the following expression for the non-local Wronskian:

$$W(r) = 1 - \frac{W_0}{k} \left\{ \int_0^\infty g(s)\mathscr{N}(s) ds \int_0^r g(t)\mathscr{J}(t) dr - \int_0^\infty g(s)\mathscr{J}(s) ds \int_0^r g(t)\mathscr{N}(t) dt \right\}. \tag{5.14}$$

The quantity $W(r) \to 1$ when $r \to 0$ or ∞. Eqs. (5.14), (5.13) and (5.6) define the ELP of the potential involved in eq. (5.5).

It remains to show that the approximation described by expression (5.2) and used for the computation of the ELP of the potential (5.1) is a good approximation. We first consider the potential

$$\mathscr{V}_2(r, r') = v_0 + iW_g^L g(r)g(r') + iW_h^L h(r)h(r'). \tag{5.15}$$

Let $v_0 + U_g(r)$ be the ELP of $v_0 + iW_g^L g(r)g(r')$. We construct the auxiliary potential

$$\mathscr{V}_{\text{aux}} = v_0 + U_g(r) + iW_h^L h(r)h(r'), \tag{5.16}$$

whose ELP can be written

$$\mathscr{V}_{\text{eq}}^{\text{aux}} = v_0 + U_g(r) + U_h(r). \tag{5.17}$$

This is not the ELP of $\mathscr{V}_2(r, r')$. Indeed, the corresponding phase shifts are given to first order in W_h^L by:

$$\tilde{\delta} = \tilde{\delta}_g + \arcsin \left\{ -\frac{2mi}{\hbar^2} W_h^L \left[\int \psi_g(r)h(r) dr \right]^2 \right\}, \tag{5.18}$$

where $\tilde{\delta}_g$ and ψ_g are the phase shift and the regular function associated with $v_0 + U_g(r)$. The phase shifts corresponding to the ELP of $\mathscr{V}_2(r, r')$ (or to $\mathscr{V}_2(r, r')$) are given

to first order in W_h^L by:

$$\delta = \delta_g + \arcsin\left\{-\frac{2mi}{\hbar^2} W_h^L \left[\int u_g(r) h(r)\,\mathrm{d}r\right]^2\right\}. \tag{5.19}$$

The quantities δ_g and $u_g(r)$ are associated with the potential $v_0 + iW_g^L g(r)g(r')$. Because of the definition of the ELP, $\tilde{\delta}_g = \delta_g$ and $u_g(r) = F_g(r)\psi_g(r)$. If the non-local part of the potential in eq. (5.1) can be considered as a small perturbation of v_0, the factor F_g is close to unity, and $\tilde{\delta}$ is equal to δ within the same approximation. In all the calculations below, $|F_g| \geqq 0.96$. Thus $\mathscr{V}_{\mathrm{eq}}^{\mathrm{aux}}(r)$ gives the ELP of $\mathscr{V}_2(r, r')$ to a very good approximation. A check of the validity of this procedure consists in inverting the terms in $g(r)$ and $h(r)$ in relation (5.2), calculating the ELP and comparing with the ELP obtained with the previous order. The relative difference which we have obtained is of the order of 10^{-3}.

We have computed the ELP of potential (5.1) with the values of W_g^L, W_h^L, W_k^L contained in table 6. Let $\mathscr{V}_{\mathrm{eq}}$ be the potential obtained in this way. We write:

$$\mathscr{V}_{\mathrm{eq}}(r) = v_0 + \overline{\mathscr{V}}(r). \tag{5.20}$$

Although the non-local part of (5.1) does not contain a spin-orbit term, the quantity $\overline{\mathscr{V}}$ depends upon both L and j, since v_0 contains a spin-orbit coupling. However, this dependence on j is very small. In the scale of fig. 4, where we plot the quantities Im $\mathscr{V}_{\mathrm{eq}}(r)$, it is not possible to distinguish between the curves for $L = 1, j = \frac{3}{2}$ and $L = 1, j = \frac{1}{2}$. For $L = 2$, $L = 3$, the difference is slightly larger but it never exceeds 0.2 MeV. The real part of $\overline{\mathscr{V}}$ is of the order of 0.1 MeV and does not significantly perturb the real part of the OMP (5.1).

5.2. COMPARISON WITH EXPERIMENT

In this subsection, we compare the results of our calculation with experiment. Since only the polarization of the scattered 14.5 MeV protons by ^{39}K has been measured experimentally and since this observable is not very sensitive to the imaginary part, we shall refer to the phenomenological OMP and the cross sections which can be derived from this potential as experimental quantities.

5.2.1. Shape of the imaginary part of the OMP. In fig. 4, we plot the shape of the imaginary part of the ELP and the shape of the imaginary part of the local OMP used by Rosen *et al.* [10]). One notices a sizable difference between theory and experiment. In particular, the theory shows less absorption at the nuclear surface and outside the nucleus, and more absorption around $r = 2.2$ fm. In fig. 5, we display the imaginary part of the ELP for $l = 0$, obtained from the effective interactions F1–F4 (see eq. (4.4)). The shape remains unchanged, although the amplitude can be enhanced for some density-dependent interactions. We shall see, however, that this does not imply big differences in the scattering properties. We also consider the volume integral $\mathscr{I}_{\mathrm{V}}$ of the imaginary part of the OMP. Our calculation leads to $\mathscr{I}_{\mathrm{V}} \approx -800$ MeV · fm^3 with a density-independent interaction. This quantity may reach $\mathscr{I}_{\mathrm{V}} \approx -1600$

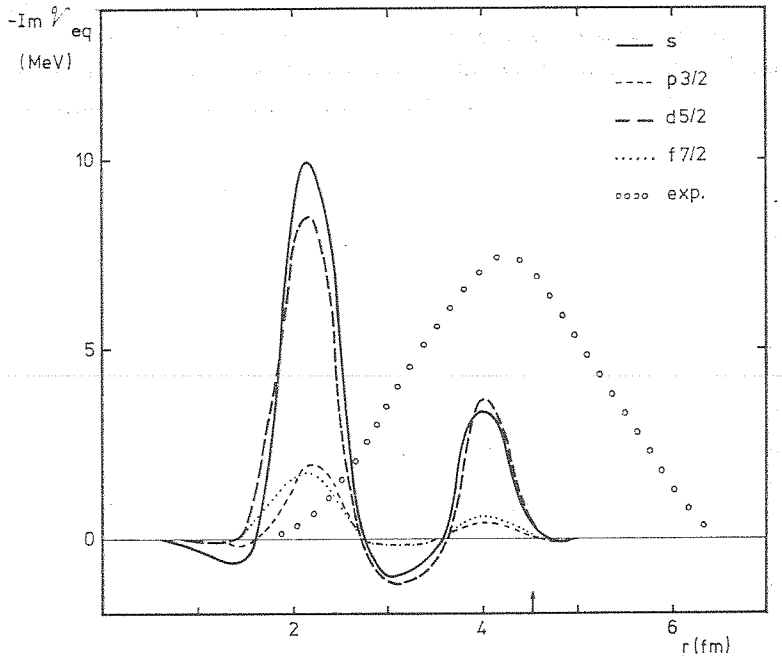

Fig. 4. Imaginary parts of equivalent local potentials, compared with the phenomenological OMP (circles) for the scattering of 14.5 MeV protons by ^{39}K. The arrow indicates the nuclear radius.

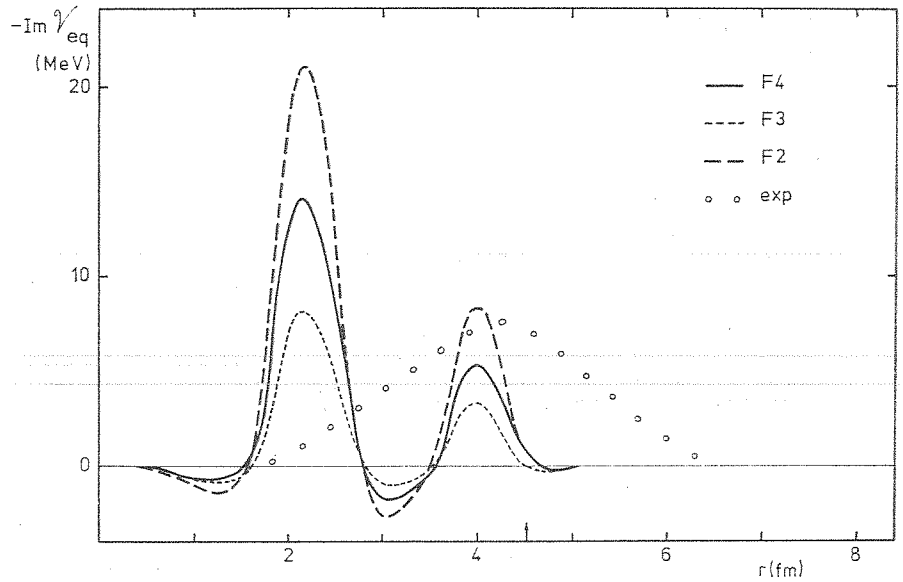

Fig. 5. ELP of the OMP computed with effective interactions F2, F3, F4. The curve corresponding to F1 cannot be distinguished from the curve for F2 in the scale of the figure.

MeV · fm^3 if density dependence is introduced in the interaction. The same quantity for the phenomenological OMP of Rosen *et al.* [10]) is equal to $\mathcal{I}_V = -4230$ MeV · fm^3. We give this comparison for the sake of completeness, since: (i) only the s-wave part is involved in this quantity; (ii) the cross sections are not very sensitive to this quantity.

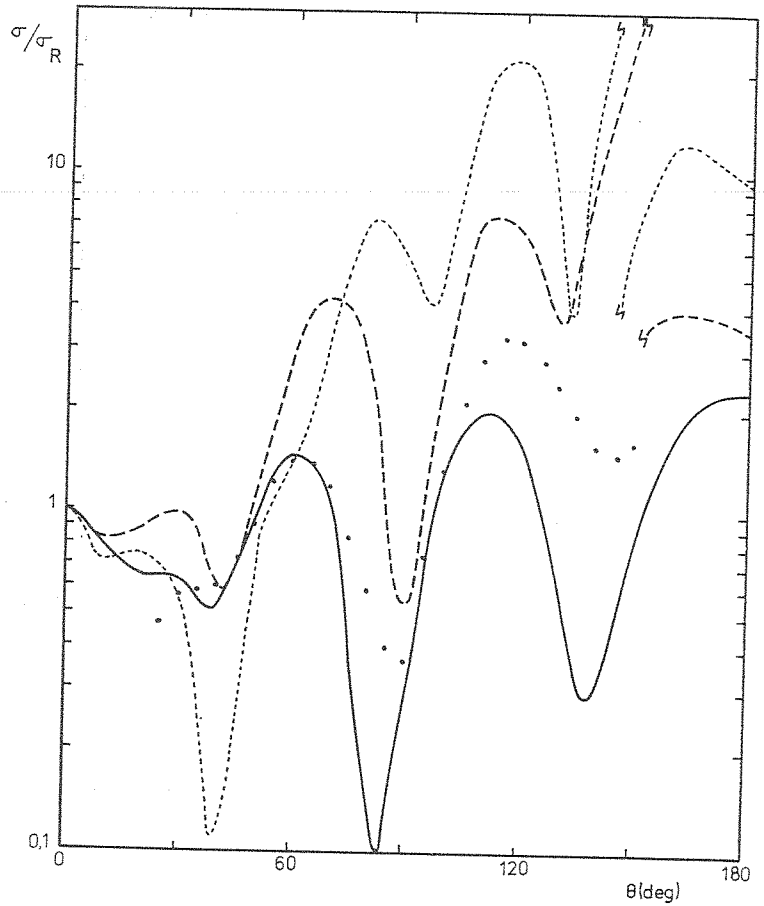

Fig. 6. Comparison of the differential cross section calculated from potential (5.20) (small dashes) with the one calculated from the potential of Rosen *et al.* [10]) (full curve) and with the average experimental data for neighbouring nuclei (dots). The curve in large dashes corresponds to the real part of the potential of Rosen *et al.* and the calculated imaginary part.

5.2.2. Elastic differential cross section. In the absence of measurements, we have taken as reference the differential cross section corresponding to the potential of Rosen *et al.* [10]), as well as the differential cross section obtained by averaging over measurements for neighbouring nuclei at the same energy. We have used the data concerning ^{40}Ca and ^{40}Ar [ref. [26])]. The comparison with the value obtained from

our ELP is illustrated by fig. 6. The discrepancy is largely due to the diffuseness parameter of ref. [15]) ($a = 0.62$ fm). If one uses for the real well the parameters of Rosen *et al.* ($a = 0.65$ fm), one finds a better agreement with the experimental data, but with still too large a value at backward angles. This seems to indicate that the absorption is too small [27]).

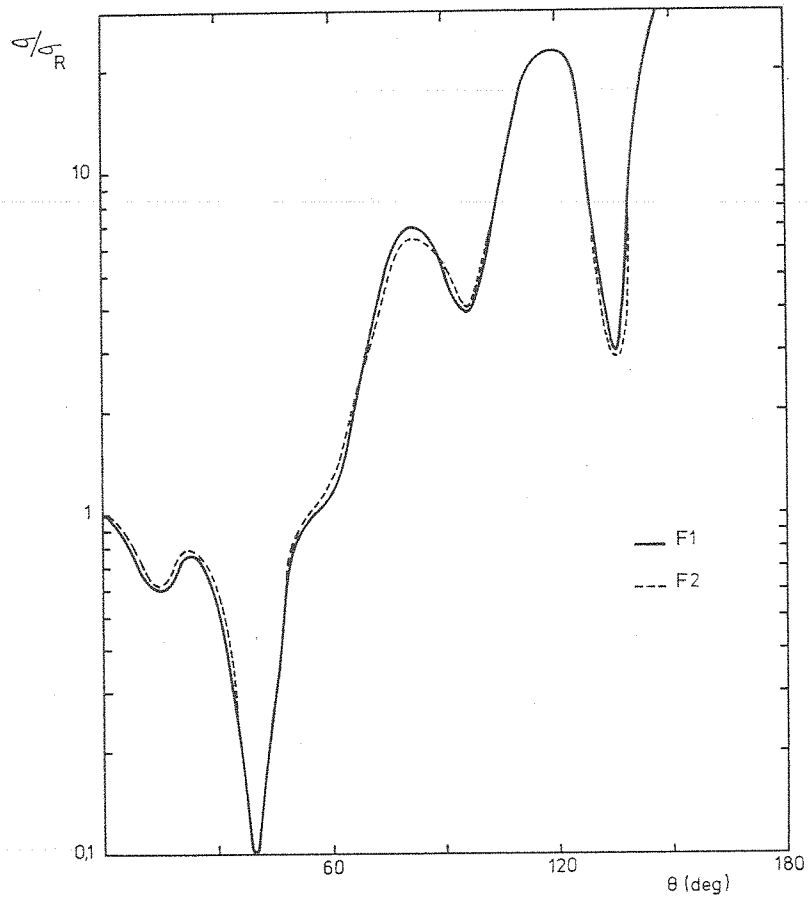

Fig. 7. Differential cross sections computed from the ELP of the OMP calculated with the interactions F1 and F2. For the sake of clarity, curves for F3 and F4 have not been drawn. They are very close to the others.

If density-dependent interactions (F1–F4) are used, one gets the results of fig. 7. We see that, although the imaginary parts are quite different, the cross sections are almost similar and very close to the one obtained in fig. 6.

5.2.3. Wave function. Absorption damps the wave function in the nuclear volume. For a local potential, the wave function can also be damped because of reflection at the nuclear surface. In order to isolate the first effect, we have compared in fig. 8 the

$l = 0$ wave functions obtained from the OMP of Rosen *et al.* and from the theoretical OMP [eq. (5.20)] with the wave function for v_0. The first two are rather similar for $r \gtrapprox 3.5$ fm, but differ for smaller values of r. This is related to the absorption predicted by the theory around 2.2 fm.

5.2.4. Absorption cross section. The absorption cross section is proportional to the loss of the incident flux. Unfortunately, there exists no measurement of this quantity for ^{39}K. However, the gross variation of the absorption cross section with the energy

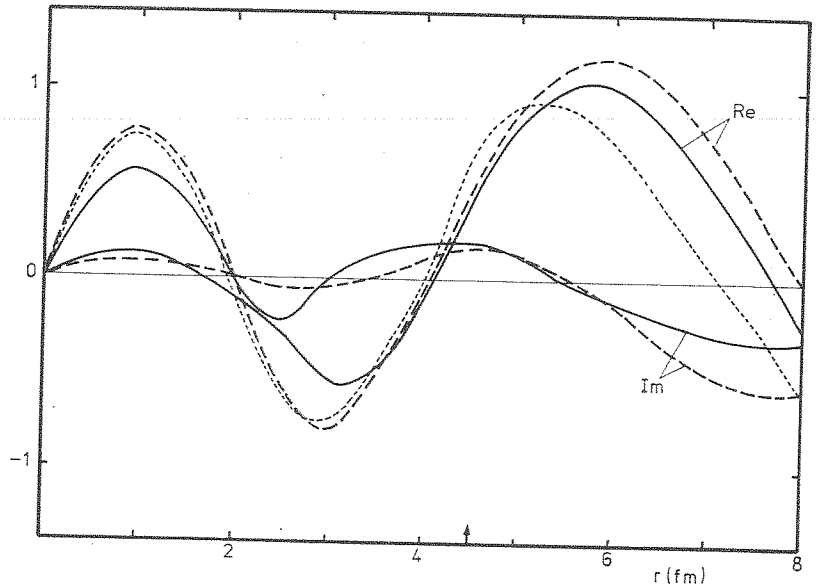

Fig. 8. Comparison of the $l = 0$ wave functions obtained from the potential (5.20) (full curve), from the phenomenological potential of Rosen *et al.* [10]) (large dashes) and from the real part of potential (5.20) (small dashes).

and the atomic number A is known [27]). In the present case, we have approximately the value $\sigma_A \approx 800$ mb. The absorption cross section found by using the phenomenological potential of Rosen *et al.* is $\sigma_A \approx 1050$ mb. The theoretical value lies around 600 mb.

6. Non-locality

We want to compare the non-locality of the imaginary part of the OMP calculated in sect. 4 with the non-locality of the Perey-Buck potential [28]):

$$\mathscr{V}_N(\tfrac{1}{2}(r+r')) \exp\left[-\left(\frac{r-r'}{b}\right)^2\right]. \qquad (6.1)$$

Let us recall the form of the imaginary part (see eqs. (2.14) and (5.1)):

$$\text{Im } \mathscr{V}^{\text{plane}}(r, r') = \sum_L \frac{2L+1}{4\pi} P_L(\cos\Theta)\{W_g^L g(r)g(r') + W_h^L h(r)h(r') + W_k^L k(r)k(r')\}. \quad (6.2)$$

In order to compute the non-locality parameter, we write this potential as a function of the quantities

$$R = \tfrac{1}{2}(r+r'), \quad \rho = r-r'. \quad (6.3)$$

Because of the rotational invariance of (6.2), the potential depends only upon R, ρ and the angle λ between the vectors R and ρ.

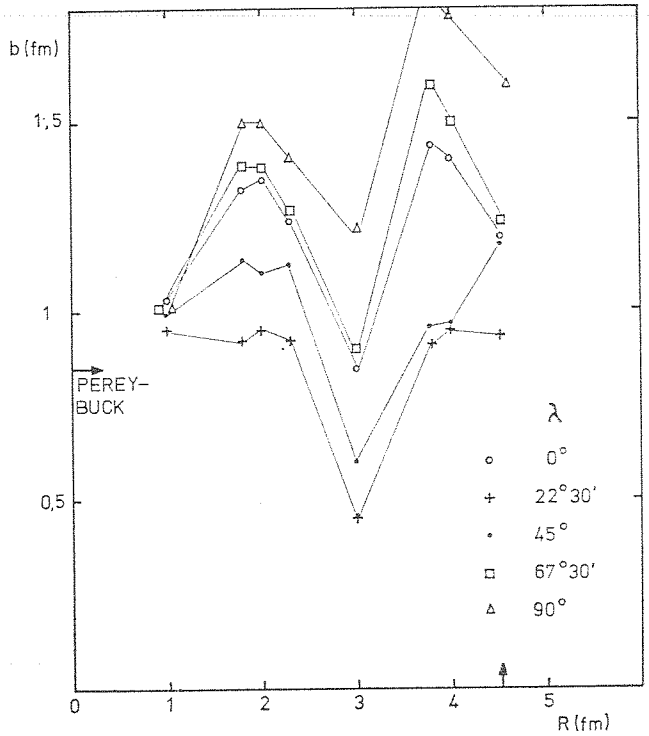

Fig. 9. Variation of the non-locality parameter b with R and λ. The horizontal arrow indicates the Perey-Buck value.

For $0 < R \lesssim 0.8$ fm, the dependence on ρ is rather complicated, but the potential (6.2) is very small in that region. For $R \gtrsim 0.8$ fm, Im $\mathscr{V}^{\text{plane}}(R, \rho, \lambda)$ behaves like $\exp(-\rho^2/b^2)$ to a fairly good approximation. The parameter b depends, however, on the value of λ. Our results are summarized in fig. 9. On the average, the non-locality is roughly equal to the value given by Perey and Buck (0.85 fm) at $R \approx 3$ fm and peaks at larger values around 2 and 4 fm. We come back to this point later on.

7. Discussion

In this section we analyse our results and make some comments concerning two aspects of these results.

7.1. LOCALIZATION OF THE ABSORPTION

Our calculations show that the imaginary part of the OMP is concentrated in two regions lying around 2.2 fm and 4 fm, respectively. This feature results from the fact that the functions g, h, k, or, equivalently the form factors $I_{cc'}$ and I_s^c, are important in these regions. Now, the form factors are the products of two single-particle wave functions (weighted by the function $u_{h_c}(r) = 1d_{\frac{3}{2}}$ which is always present in the form factors), one corresponding to a single-particle state in the $N = 2$ shell (2s, 1d) and the other to a single-particle state in the $N = 3$ shell (1f, 2p) and $N = 4$ shell (3s, 2d) (in the continuum). The form factors are important when the overlap between the single-particle wave functions is important, or, roughly speaking, when the overlap between the matter density functions in the $N = 2$ shell, on the one hand, and in the $N = 3, 4$ shells, on the other hand, is important. This happens at 2 and 4 fm. It thus appears that the radial dependence of the theoretical imaginary part of the OMP is largely govenered by shell effects. The maxima of the non-locality parameter, observed in fig. 9, may be interpreted in the same way.

Some results obtained by other authors can be understood along these lines. For instance, Slanina [6]) computed the imaginary part of the OMP for ^{40}Ca+p. This work differs from ours in the sense that he neglects the compound nucleus contribution, and he uses a more sophisticated description of the target in the inelastic channels. He finds an absorption concentrated around 4 fm, while the nuclear radius is 4.30 fm. This bump corresponds to the transition between major shells $N = 2$ to $N = 3, 4$. However, he does not find any absorption peak around 2 fm. This may be due to the interaction used (the Green force) or to the approximations made to build the ELP. Slanina has also computed the OMP for the case ^{12}C+p. There, the situation is more clear. The imaginary part peaks at 2 fm [ref. [6])], while the nuclear radius is 2.9 fm. This zone results from the overlap between the matter density functions for $N = 1$ and $N = 2, 3$ shells.

The calculation by Bruneau and Vinh Mau [5]) for the ^{40}Ca+p system is similar to that of Slanina (except for the construction of the ELP). They find a strong absorption between 1 and 2 fm, presumably connected with the overlap between matter density in the $N = 2$ and $N = 3, 4$ shells.

7.2. IMPORTANCE OF THE ABSORPTION

From subsect. 5.2 it emerges that the absorption is too small. The absorption cross section shows that there is a lack of absorption of about 40 %. This difference between experimental and theoretical absorptions may arise from the theoretical description of the target states in the inelastic channels. It was our hope in choosing ^{39}K as a target, that the states should be well described by shell-model configurations,

or at least, that those states which are well described by the shell model are the most important for the absorption. This calculation shows that this is only partly true. Other more complicated inelastic channel states must be included. It is now evident that some excited states in ^{39}K are due to the coupling of a hole to some vibrational quanta of the ^{40}Ca core [29]). The influence of the addition of inelastic channels corresponding to those target states on the absorption have been included very briefly in ref. [12]). Most of the discrepancy between theory and experiment can be removed by the addition of those states. This will be discussed in a forthcoming paper [30]).

8. Conclusion

We have shown that the compound nucleus contribution to the absorption is appreciable, at energies up to those considered here (14 MeV). This contribution depends upon energy and angular momentum.

The phenomenological concentration of the imaginary part of the OMP at the nuclear surface is only a convenient hypothesis for analysing the experimental cross sections and is not supported by the theory. We have found, as other authors, that the imaginary part extends throughout the nuclear volume, and that, for magic or near magic nuclei, the distribution of the imaginary part undergoes strong shell effects. Collective excitations probably enhance the absorption at the nuclear surface, since they can be viewed as vibrations of the nuclear surface. The importance of collective excitations, as far as absorption is concerned, has been studied by O'Dwyer *et al.* [7]) in a particle-vibration coupling model. Unfortunately, they do not discuss the radial dependence of the imaginary part of the OMP. However, it is our feeling that these collective excitations cannot destroy completely the distribution of the absorption determined by the underlying shell structure.

We want to thank Prof. C. Mahaux for his encouragements and for many stimulating discussions. We are also grateful to Dr. J. P. Jeukenne for his aid in the numerical work.

Appendix

OPTICAL POTENTIAL FOR AN INCIDENT PLANE WAVE

Let $\mathscr{V}_E^{\mathrm{opt}(c)}$ be the OMP in an elastic channel specified by the quantum numbers $c = \{ljIJT_cM_{T_c}TM_T\}$, which are respectively the orbital and total angular momenta of the incident nucleon, the spin of the target, the total spin of the system, the isospin of the target and the total isospin of the system. We first want to construct the OMP acting on an incident plane wave.

We write it as:

$$\mathscr{V}^{\mathrm{opt}} = v_0 + \mathscr{V}(r, r') + \mathscr{V}_{\mathrm{s.o.}}(r, r')\boldsymbol{l}\cdot\boldsymbol{s} + \mathscr{V}_{\mathrm{SS}}(r, r')\boldsymbol{j}\cdot\boldsymbol{I} + \mathscr{V}_{\mathrm{TT}}(r, r')\boldsymbol{t}\cdot\boldsymbol{T}_c, \quad \text{(A.1)}$$

where s is the spin of the incident nucleon and t its isospin. It is easy to see that a Schrödinger equation for potential (A.1) can be reduced to a certain number of independent radial equations like (2.5). One has with obvious notation

$$\tilde{\mathscr{V}}^{c=\{LjIJT_cMT_cTM_T\}} = \mathscr{V}_L(r,r')+\tfrac{1}{2}[j(j+1)-L(L+1)-\tfrac{3}{4}]\mathscr{V}_L^{\text{s.o.}}(r,r')$$
$$+\tfrac{1}{2}[J(J+1)-j(j+1)-I(I+1)]\mathscr{V}_L^{\text{SS}}(r\ r')+\tfrac{1}{2}[T(T+1)-T_c(T_c+1)-\tfrac{3}{4}]\mathscr{V}_L^{\text{TT}}(r,r'). \tag{A.2}$$

In this paper, we are interested in the inverse problem, namely to start from the quantities $\tilde{\mathscr{V}}^c$ in order to calculate the quantities $\mathscr{V}_L$, $\mathscr{V}_L^{\text{s.o.}}$. Thus, we invert the system of equations obtained in writing eq. (A.2) for all possible values of the quantum numbers. Let us show that in the simple case where spin-orbit and spin-spin terms are neglected (except for a spin-orbit term which could be included in v_0), and where only the diagonal term in isospin space is retained, a simple formula can be obtained. Then, the OMP can be written as:

$$\mathscr{V}^{\text{opt}} = v_0+\mathscr{V}^{\text{plane}}(\boldsymbol{r},\boldsymbol{r}'), \tag{A.3}$$

with

$$\mathscr{V}^{\text{plane}}(\boldsymbol{r},\boldsymbol{r}') = \mathscr{V}(\boldsymbol{r},\boldsymbol{r}')+\mathscr{V}_{\text{TT}}(\boldsymbol{r},\boldsymbol{r}')t_z T_{c_z}, \tag{A.4}$$

$$\mathscr{V}^{\text{plane}}(\boldsymbol{r},\boldsymbol{r}') = \sum_L \frac{2L+1}{4\pi}\overline{\mathscr{V}}_L(r,r')P_L(\cos\Theta), \tag{A.5}$$

with

$$\overline{\mathscr{V}}_L(r,r') = \mathscr{V}_L(r,r')+\mathscr{V}_L^{\text{TT}}(r,r')t_z T_{c_z}. \tag{A.6}$$

We now show that $\overline{\mathscr{V}}_L$ can be written as:

$$\overline{\mathscr{V}}_L = \sum_j (L0\tfrac{1}{2}\tfrac{1}{2}|j\tfrac{1}{2})^2(2I+1)^{-1}\sum_{\mu_I}\sum_J (j\tfrac{1}{2}I\mu_I|J\mu_I+\tfrac{1}{2})^2$$
$$\times\sum_T (\tfrac{1}{2}m_t\,T_c M_{T_c}|TM_T)^2\tilde{\mathscr{V}}^{c=\{LjIJT_cM_{Tc}TM_T\}}. \tag{A.7}$$

Let us first neglect the isospin. We have, with the help of (A.2),

$$\overline{\mathscr{V}}_L = \mathscr{V}_L+\sum_j (L0\tfrac{1}{2}\tfrac{1}{2}|j\tfrac{1}{2})^2\{\tfrac{1}{2}[j(j+1)-L(L+1)-\tfrac{3}{4}]\mathscr{V}_L^{\text{s.o.}}(r,r')$$
$$+(2I+1)^{-1}\sum_{\mu_I}\sum_J (j\tfrac{1}{2}I\mu_I|J\mu_I+\tfrac{1}{2})^2\tfrac{1}{2}[J(J+1)-j(j+1)-I(I+1)]\mathscr{V}_L^{\text{SS}}(r,r')\}. \tag{A.8}$$

With obvious notation, we have:

$$\sum_{\mu_I}\sum_J (j\tfrac{1}{2}I\mu_I|J\mu_I+\tfrac{1}{2})^2\tfrac{1}{2}[J(J+1)-j(j+1)-I(I+1)] = \sum_{\mu_I}\sum_J \langle\mathscr{Y}^{\frac{1}{2}}_{Lj\frac{1}{2}}\Xi_I^{\mu_I}|X_{jJI}^{\mu_I+\frac{1}{2}}\rangle$$
$$\times\langle X_{jJI}^{\mu_I+\frac{1}{2}}|\boldsymbol{j}\cdot\boldsymbol{I}|X_{jJI}^{\mu_I+\frac{1}{2}}\rangle\langle X_{jJI}^{\mu_I+\frac{1}{2}}|\mathscr{Y}^{\frac{1}{2}}_{Lj\frac{1}{2}}\Xi_I^{\mu_I}\rangle, \tag{A.9}$$

since $\boldsymbol{j}\cdot\boldsymbol{I}$ is diagonal in the basis of X^M_{jJI}. For the same reason, we can give (A.9) the following form:

$$\sum_{\mu_I}\sum_{\substack{J,M\\J',M'}}\langle\mathscr{Y}^{\frac{1}{2}}_{Lj\frac{1}{2}}\Xi^{\mu_I}_I|X^M_{jJI}\rangle\langle X^M_{jJI}|\boldsymbol{j}\cdot\boldsymbol{I}|X^{M'}_{jJ'I}\rangle\langle X^{M'}_{jJ'I}|\mathscr{Y}^{\frac{1}{2}}_{Lj\frac{1}{2}}\Xi^{\mu_I}_I\rangle$$
$$=\sum_{\mu_I}\langle\mathscr{Y}^{\frac{1}{2}}_{Lj\frac{1}{2}}\Xi^{\mu_I}_I|\boldsymbol{j}\cdot\boldsymbol{I}|\mathscr{Y}^{\frac{1}{2}}_{Lj\frac{1}{2}}\Xi^{\mu_I}_I\rangle=\sum_{\mu_I}\tfrac{1}{2}\mu_I=0. \qquad (A.10)$$

Then, (A.8) reduces to:

$$\overline{\mathscr{V}}_L=\mathscr{V}_L+\sum_j(L0\tfrac{1}{2}\tfrac{1}{2}|j\tfrac{1}{2})^2\tfrac{1}{2}[j(j+1)-L(L+1)-\tfrac{3}{4}]\mathscr{V}^{\mathrm{s.o.}}_L(r,r'). \qquad (A.11)$$

By using the same arguments as above, we get:

$$\overline{\mathscr{V}}_L=\mathscr{V}_L. \qquad (A.12)$$

When isospin is taken into account, formula (A.7) reduces to

$$\overline{\mathscr{V}}_L=\mathscr{V}_L+m_t M_{T_c}\mathscr{V}^{\mathrm{TT}}_L, \qquad (A.13)$$

which is equivalent to (A.6).

References

1) A. M. Lane and C. F. Wandel, Phys. Rev. **98** (1955) 1524
2) L. C. Gomes, Phys. Rev. **116** (1959) 1226
3) K. Harada and N. Oda, Prog. Theor. Phys. **21** (1959) 260
4) G. L. Shaw, Ann. of Phys. **8** (1954) 509
5) M. Bruneau and N. Vinh Mau, Methods and problems of theoretical physics, ed. J. E. Bowcock (North-Holland, Amsterdam, 1970) p. 333
6) D. A. Slanina, thesis, Michigan University, 1971, unpublished
7) T. F. O'Dwyer, M. Kawai and G. E. Brown, Phys. Lett. **41B** (1972) 259
8) F. L. Friedman and V. F. Weisskopf, Niels Bohr and the development of physics, ed. W. Pauli (Pergamon, London, 1955) p. 134
9) C. Mahaux and H. A. Weidenmüller, Shell-model approach to nuclear reactions (North-Holland, Amsterdam, 1969)
10) L. Rosen *et al.*, Ann. of Phys. **34** (1965) 96
11) R. Lipperheide, Nucl. Phys. **89** (1966) 97
12) J. Cugnon, thesis, 1972
13) F. Ajzenberg-Selove and T. Lauritsen, Nucl. Phys. **11** (1959) 1
14) V. Gillet and E. A. Sanderson, Nucl. Phys. **54** (1964) 472
15) K. Takeuchi and P. A. Moldauer, Phys. Lett. **28B** (1969) 384
16) G. E. Brown, L. Castillejo and J. A. Evans, Nucl. Phys. **22** (1961) 1
17) J. W. Negele, Phys. Rev. **C1** (1970) 1260
18) S. A. Moszkowski, Proc. Symp. on nuclear structure, Dubna (IAEA, Vienna, 1968)
19) K. R. Lassey and A. R. Volkov, Phys. Lett. **36B** (1971) 4
20) R. M. Lemmer and C. M. Shakin, Ann. of Phys. **27** (1964) 13
21) G. L. Payne, Phys. Rev. **174** (1968) 1227
22) A. M. Davidson, Nucl. Phys. **A180** (1972) 208
23) H. Fiedeldey, Nucl. Phys. **A96** (1967) 463
24) M. Coz, A. D. McKellar and L. G. Arnold, Ann. of Phys. **58** (1970) 504
25) R. G. Newton, Scattering theory of waves and particles (McGraw-Hill, New York, 1966) ch. 12
26) W. S. Gray *et al.*, Nucl. Phys. **67** (1965) 542
27) P. E. Hodgson, The optical model of elastic scattering (Clarendon Press, Oxford, 1963)
28) P. Perey and B. Buck, Nucl. Phys. **32** (1962) 353
29) S. Wiktor, Phys. Lett. **40B** (1972) 181
30) J. Cugnon, to be published